JOURNAL OF Materials CHEMISTRY

Synthesis, structures and two-photon pumped up-conversion lasing properties of two new organic salts

Yan Ren,[a] Qi Fang,*[a] Wen-Tao Yu,[a] Hong Lei,[a] Yu-Peng Tian,[a] Min-Hua Jiang,[a] Qing-Chuan Yang[b] and Thomas C. W. Mak[b]

[a]*State Key Laboratory of Crystal Materials, Shandong University, Jinan, 250100, P.R. China. E-mail: fangqi@icm.sdu.edu.cn; Fax: 86-531-8565403*
[b]*Department of Chemistry, The Chinese University of Hong Kong, P.R. China*

Received 8th February 2000, Accepted 6th June 2000
Published on the Web 1st August 2000

We have synthesized two new organic salts, *trans*-4-[*p*-(*N*-hydroxyethyl-*N*-methylamino)styryl]-*N*-methylpyridinium toluene-*p*-sulfonate (abbreviated as HMASPS) and *trans*-4-[*p*-(*N*-hydroxyethyl-*N*-ethylamino)styryl]-*N*-methylpyridinium toluene-*p*-sulfonate (abbreviated as HEASPS). X-Ray diffraction analyses reveal that HMASPS crystal belongs to the $P2_1/n$ space group, with water molecules co-crystallized in the crystal and forming the monohydrate with the formula of $C_{17}H_{21}N_2O^+ \cdot C_7H_7O_3S^- \cdot H_2O$, while HEASPS belongs to the $P\bar{1}$space group, with no solvent molecules. Pumped by a 1064 nm, 50 ps laser pulse at 2.02 mJ input energy, an up-conversion lasing of 0.169 mJ output energy can be obtained with 0.05 M HMASPS–DMF solution, and the output/input efficiency is 8.4%. A 0.05 M HEASPS–DMF solution exhibits a lasing efficiency of 9.1% with input and output energy of 1.90 mJ and 0.173 mJ respectively.

Introduction

Two-photon absorption (TPA) is a process by which two photons are simultaneously absorbed to an excited state in a medium *via* a virtual state. TPA intensity is characterized by the TPA cross section. Materials with a large TPA cross section have received considerable attention in recent years because of their interesting frequency up-conversion mechanism and potential applications in three-dimensional fluorescence imaging,[1] optical data storage,[2–4] lithographic microfabrication,[4–6] laser device fabrication[7–13] and photodynamic therapy.[14] The two-photon pumped (TPP) up-conversion materials used as laser media have the advantage that they can be pumped at longer wavelengths where the organic dyes are relatively photostable, and semiconductor diode lasers may be used as pump sources. Moreover when they are pumped at longer wavelengths, Rayleigh scattering and linear absorption are greatly reduced. In contrast to second harmonic based frequency up-conversion, TPA is a third order nonlinear optical process, based on which the corresponding up-conversion emission has no limitation on molecular centrosymmetry, and in principle a wide variety of molecules could be chosen for luminescence material exploration. There is also no crystalline centrosymmetry limitation, so TPA based up-conversion emission can be easily performed in solution and in various isotropic glass states as well as in anisotropic crystalline states. TPP up-conversion lasing efficiency is one of the basic criteria in lasing device fabrication, and those materials with high lasing efficiency are now in great demand. Although quite a large family of TPA active molecules has been discovered, there are only about a dozen organic molecules reported to have remarkable TPP up-conversion lasing properties. Among them, only a few have satisfactorily high lasing efficiencies.

In exploring strong TPA compounds, Albota *et al.* have focused on symmetric intramolecular charge transfer organic molecules,[15] and Reinhardt *et al.* have emphasized the asymmetric intramolecular charge transfer ones.[16] Up till now, the correlation between structure and TPA properties has not been well understood, and also very little is known about the excited state related to TPP up-conversion emission. On the other hand, as a rule of thumb, most TPP lasing molecules are large polar π-conjugated systems with excellent planar molecular configuration and donor–acceptor substituents. These structural characteristics are similar to those of second order nonlinear optically active molecules. Obviously, the electron delocalization in these molecules contributes to the enhancement of the TPA cross section; the polarity, we believe, is also important for TPP up-conversion lasing. He *et al.* have reported seven lasing dyes (named as ASPT,[7] ASPI,[8] M-PPE,[9] DHASI,[10] DAST,[11] APSS[12] and Coumarin,[13] respectively). All of them possess high polarity.

Based on the above considerations, we have synthesized two new organic salts, HMASPS and HEASPS, and the toluene-*p*-sulfonate anion has been chosen as counterion because it is also a planar π-conjugated and highly polar system. X-Ray structure determinations for both HMASPS and HEASPS have been carried out. The linear and nonlinear optical properties including linear absorption, single-photon and two-photon excited fluorescence and two-photon pumped lasing behavior for HMASPS and HEASPS in solution are presented in this article.

Experimental

1 Synthesis

Elemental analysis data were obtained using a Heraeus Rapid CHNO elemental analyzer. Nuclear magnetic resonance experiments were performed on an INOVA-300 spectrometer. Infrared spectra were recorded on a Nicolet 20SX FT-IR spectrometer. Thermal analyses were performed on a Perkin Elmer TGS-2 thermogravimetric analyzer.

4-(*N*-Methyl-*N*-hydroxyethylamino)benzaldehyde (1). Compound **1** and 4-(*N*-ethyl-*N*-hydroxyethylamino)benzaldehyde (**2**) were synthesized according to reference 17. At room temperature, compound **1** is a pale yellow solid, and compound **2** is a brown oil. 1,4-Dimethylpyridinium iodide (**3**) was synthesized as a white powder according to reference 7 (see Scheme 1).

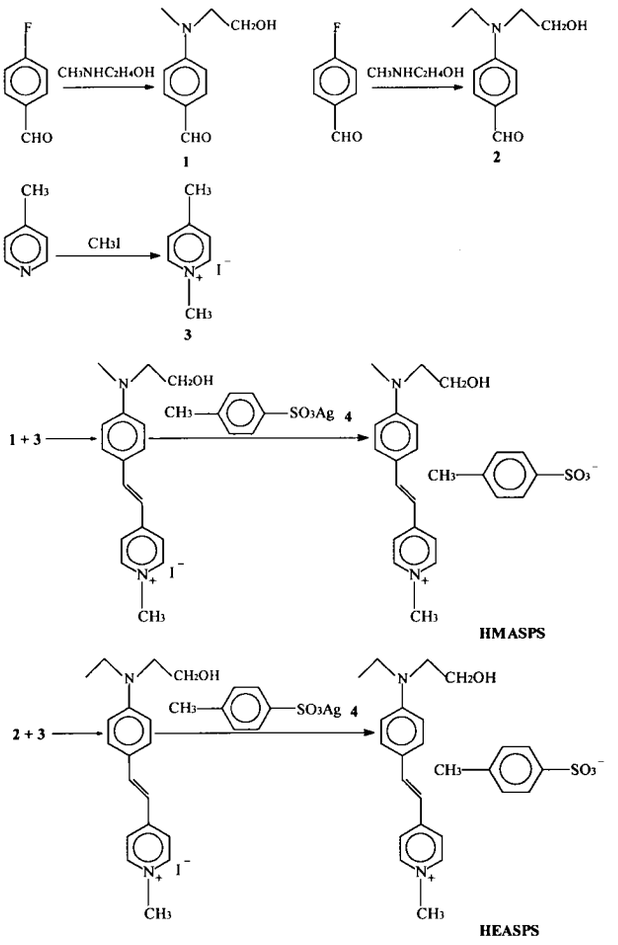

Scheme 1

Silver toluene-*p*-sulfonate (4). 34 g (0.2 mol) silver nitrate was dissolved in 100 mL distilled water, then mixed with a solution of 10.6 g (0.1 mol) Na_2CO_3 in 100 mL water. The as-formed Ag_2CO_3 precipitate was washed with water repeatedly and removed into a beaker containing a stirrer and 200 mL distilled water. Then 38 g (0.2 mol) of toluene-*p*-sulfonic acid monohydrate were added to the beaker in portions with heating and stirring over the course of 1 h. After removing some insoluble impurities by filtration, the hot transparent solution was allowed to stand until colorless parallelepiped crystals were formed in the course of natural cooling and evaporation. 52.2 g product was obtained in all, yield 93%.

***trans*-4-[*p*-(*N*-Hydroxyethyl-*N*-methylamino)styryl]-*N*-methylpyridinium toluene-*p*-sulfonate (HMASPS).** 4.66 g (0.026 mol) of compound **1**, 6.20 g (0.026 mol) of compound **3**, and 100 mL of acetonitrile were added into a 250 mL one-necked flask fitted with a stirrer and a condenser. Then four drops of piperidine were added. The solution was heated to reflux at 80 °C for four hours to form the *trans*-4-[*p*-(*N*-hydroxyethyl-*N*-methylamino)styryl]-*N*-methylpyridinium cation. This solution was added into a solution of 7.25 g (0.026 mol) silver toluene-*p*-sulfonate in 100 mL acetonitrile with stirring and heating simultaneously in a one-necked flask, followed by refluxing for about two hours. Then the stirring was continued at room temperature overnight. The silver iodide precipitate was filtered off. During evaporation of the clear red solution, shining microcrystals formed. The product was recrystallized from acetonitrile and purple-red parallelepiped crystals that could be used for X-ray structure determination were obtained. The crystal structure analysis reveals that a water molecule is co-crystallized with the HMASPS salt. This result has been confirmed by TGA and DTA thermal analyses. Calcd for $C_{24}H_{28}N_2O_4S{\cdot}H_2O$: C, 62.86; H, 6.54; N, 6.11. Found: C, 62.87; H, 6.64; N, 5.96%. IR spectrum (KBr) ν/cm^{-1}: 1577.8s, 1525.9s, 1384.9m, 1343.1m, 1221.9m, 1172.5s, 1121.2m, 1071.3m, 1034.5m, 1011.1m, 678.9m, 567.8m. ^{1}H NMR (DMSO-d_6) (300 MHz; TMS) δ_H: 2.27 (3H, s), 3.02 (3H, s), 3.36 (1H, s), 3.49 (2H, t, *J* 5.2 Hz), 3.55 (2H, q, *J* 5.2 Hz), 6.78 (2H, d, *J* 8.6 Hz), 7.09 (2H, d, *J* 7.4 Hz), 7.13 (1H, d, *J* 14.3 Hz), 7.46 (2H, d, *J* 7.9 Hz), 7.55 (2H, d, *J* 8.6 Hz), 7.88 (1H, d, *J* 15.9 Hz), 8.01 (2H, d, *J* 6.3 Hz), 8.65 (2H, d, *J* 6.5 Hz).

***trans*-4-[*p*-(*N*-Hydroxyethyl-*N*-ethylamino)styryl]-*N*-methylpyridinium toluene-*p*-sulfonate (HEASPS).** Following the same procedure as mentioned above, HEASPS was synthesized using 5.0 g (0.026 mol) of compound **2**, 6.2 g (0.026 mol) of compound **3** and 7.25 g (0.026 mol) of silver toluene-*p*-sulfonate in 100 mL acetonitrile. The silver iodide precipitate was filtered off from the solution. During the slow evaporation of the clear red filtrate, purple-red parallelepiped crystals were isolated. Calcd for $C_{25}H_{30}N_2O_4S$: C, 66.05; H, 6.60; N, 6.16. Found: C, 65.65; H, 6.63; N, 5.86%. IR spectrum (KBr) ν/cm^{-1}: 1642.3m, 1581.5s, 1521.7s, 1398.7m, 1224.5m, 1170.1s, 1122.5m, 1057.8m, 1029.7m, 1008.4m, 826.7s, 680.0s, 569.6s. ^{1}H NMR(DMSO-d_6) (300 MHz; TMS) δ_H: 1.11 (3H, t, *J* 6.8 Hz), 2.29 (3H, s), 3.36 (1H, s), 3.56 (2H, q, *J* 5.5 Hz), 4.16 (3H, s), 6.78 (2H, d, *J* 9.2 Hz), 7.11 (2H, d, *J* 7.7 Hz), 7.14 (1H, d, *J* 7.7 Hz), 7.47 (2H, d, *J* 8.1 Hz), 7.56 (2H, d, *J* 9.2 Hz), 7.89 (1H, d, *J* 16.5 Hz), 8.02 (2H, d, *J* 6.6 Hz), 8.66 (2H, d, *J* 6.6 Hz).

The TGA curve of HMASPS shows that there is a 3.61% weight loss in the heating process from 72 °C to 143 °C, which was proved to be the water of hydration by X-ray structure determination. The DTA curve of HMASPS indicates that the temperature at which the water of hydration is lost is 126 °C. The melting point of HMASPS is 186 °C, and it decomposes at temperatures above 304 °C. In the TGA and DTA experiments, no obvious weight loss was found for HEASPS before its melting point. HEASPS melts at 198 °C and decomposes at 338 °C. The results of the above thermal analyses indicate that both compounds are thermally and chemically stable, and may be photostable enough to undergo fairly strong laser pulses.

2 Structure determination†

The X-ray diffraction data for HMASPS were collected on a Rigaku R-AXIS C IP diffractometer by the IP method and those for HEASPS on a Bruker P4 four-circle diffractometer (Tables 1 and 2 and Figs. 1–4). By using SHELXL-97 programs, their structures were solved by direct methods and refined by full-matrix least-squares on F^2. Anisotropic displacement parameters were refined for all non-hydrogen atoms. The hydrogen atoms were not included in the structure-factor calculations.

3 Linear absorption spectra

The UV–visible–near-IR spectra were measured on a Hitachi U-3500 UV–vis–IR recording spectrophotometer by using quartz cuvettes of 1 cm path length. Both HMASPS and HEASPS show excellent solubility in many common solvents such as water, methanol, ethanol, THF, DMF, acetonitrile, benzene, toluene, chlorobenzene and benzyl alcohol *etc.* Ethanol was chosen as the solvent for recording the spectra because of its excellent UV transparency. The concentration for both solutions of HMASPS–ethanol and HEASPS–ethanol were fixed to 1.00×10^{-5} M.

From Fig. 5, one can see that the absorption behaviors of

†CCDC reference number 1145/225. See http://www.rsc.org/suppdata/jm/b0/b001058h/ for crystallographic files in .cif format.

Table 1 Crystal data, diffraction data, and refinement data of HMASPS and HEASPS

Compound	HMASPS	HEASPS
Formula	$C_{17}H_{21}N_2O^+ \cdot C_7H_7O_3S^- \cdot H_2O$	$C_{18}H_{23}N_2O^+ \cdot C_7H_7O_3S^-$
Formula weight	458.57	454.58
Crystal system	Monoclinic	Triclinic
Space group	$P2_1/n$	$P\bar{1}$
Absorption coefficient	0.176 mm^{-1}	0.173 mm^{-1}
Final R indices [$I>2\sigma(I)$]	$R=0.0776$, $wR=0.2303$	$R=0.0573$, $wR=0.1832$
a/Å	9.929 (2)	9.4237 (8)
b/Å	19.549 (4)	9.6976 (8)
c/Å	12.100 (2)	13.2841 (9)
α/°	90	86.655 (6)
β/°	96.11 (3)	74.064 (5)
γ/°	90	85.891 (7)
Cell volume/$Å^3$	2335.3 (8)	1163.40 (16)
Temperature/K	294	298
Z	4	2
λ of Mo-Kα/Å	0.71073	0.71073
Measured reflections	3581	4929
Independent reflections	3581	4111
R_{int}	0.000	0.023

these two compounds are almost the same. The two curves show that the longest wavelength UV absorption peaks are located at 483 nm for HMASPS (with the corresponding mole absorption coefficient $\varepsilon_{max}=4.0\times10^4$), and 487 nm for HEASPS (with the corresponding $\varepsilon_{max}=4.3\times10^4$). There is no reasonable linear absorption in the spectral range from 600 to 2000 nm.

Results and discussion

1 Structural features

As mentioned above, HMASPS has been identified as a monohydrate. The co-crystallized water molecules can be seen in Fig. 1 (only the oxygen of water is drawn). Various hydrogen bonds can also be seen in Fig. 1, such as the H···O bonding between the hydrogen of the hydroxy group and the oxygen of the sulfonate group, between the hydrogen of water and the oxygen of the sulfonate group, and between the hydrogen of water and the oxygen of the hydroxy group. From Fig. 3, one can also see that a kind of hydrogen bond between the hydrogen of the hydroxy group and the oxygen of the sulfonate group exists in the HEASPS crystal. By comparison, hydrogen bonding is more abundant in HMASPS than in HEASPS. Compared to HEASPS, HMASPS possesses superior crystalline habits, such as ease of crystallization from solution and ease of growing into a large three-dimensional crystal. This reveals that water related hydrogen bonding plays an important part in the crystalline process and the crystalline morphology.

From Fig. 2 and Fig. 4, one can see that the HMASPS cation and the HEASPS cation are almost perfectly planar. In fact, the maximum atomic distances to their corresponding molecular least square planes are no more than 0.1 Å. The bond lengths of the benzene ring and the pyridinium ring in both HMASPS and HEASPS are all of aromatic character. The bridge bond lengths of C4–C7–C8–C9 of HEASPS are also highly conjugated. The planar and the conjugated geometric configuration reveal that the HEASPS cation has a highly delocalized π-electron system. The bonds of the HMASPS cation plane are also conjugated, except that the same bridge linkage of C4–C7–

Table 2 The selected bond lengths (Å) of HMASPS and HEASPS

HMASPS		HEASPS	
S1–O2	1.4466(11)	S1–O1	1.443(3)
S1–O3	1.4360(13)	S1–O2	1.450(3)
S1–O4	1.4374(13)	S1–O3	1.448(2)
S1–C21	1.7659(15)	S1–C23	1.777(3)
N1–C1	1.3515(19)	O4–C18	1.391(6)
N1–C15	1.4581(18)	C2–C3	1.361(5)
N1–C17	1.451(2)	C3–C4	1.393(4)
N2–C11	1.338(2)	C4–C7	1.452(4)
N2–C12	1.3478(19)	C4–C5	1.397(5)
N2–C14	1.465(2)	C5–C6	1.368(5)
O1–C16	1.416(2)	C7–C8	1.340(4)
C1–C2	1.4067(19)	C8–C9	1.451(4)
C1–C6	1.418(2)	C9–C10	1.396(4)
C2–C3	1.346(2)	C9–C14	1.390(5)
C3–C4	1.377(3)	C10–C11	1.376(4)
C4–C5	1.386(3)	C11–C12	1.389(4)
C4–C7	1.665(3)	C12–C13	1.412(5)
C5–C6	1.370(2)	C13–C14	1.370(5)
C7–C8	1.115(3)	C15–C16	1.505(6)
C8–C9	1.674(3)	C17–C18	1.542(6)
C9–C10	1.396(3)	C19–C20	1.505(5)
C9–C13	1.347(3)	C20–C21	1.392(5)
C10–C11	1.397(2)	C20–C25	1.375(5)
C12–C13	1.340(2)	C21–C22	1.378(4)
C15–C16	1.496(2)	C22–C23	1.382(4)
C18–C19	1.370(2)	C23–C24	1.393(4)
C18–C23	1.380(2)	C24–C25	1.391(4)
C18–C24	1.507(2)	N1–C2	1.343(5)
C19–C20	1.391(2)	N1–C1	1.482(5)
C20–C21	1.382(2)	N1–C6	1.336(5)
C21–C22	1.381(2)	N2–C12	1.380(4)
C22–C23	1.386(2)	N2–C17	1.455(5)
		N2–C15	1.475(5)

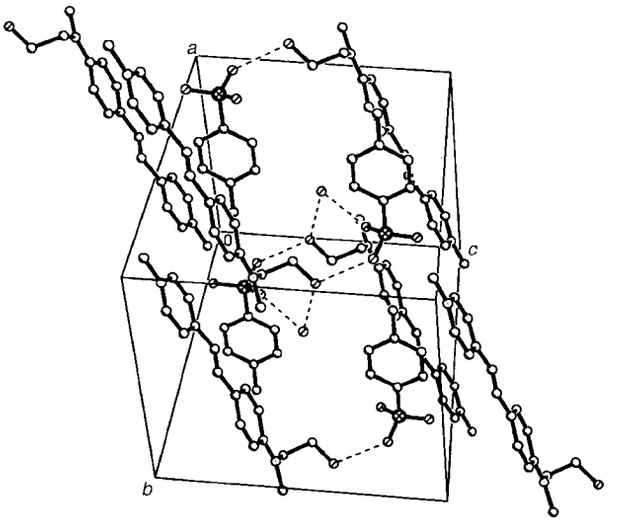

Fig. 1 Packing diagram for HMASPS.

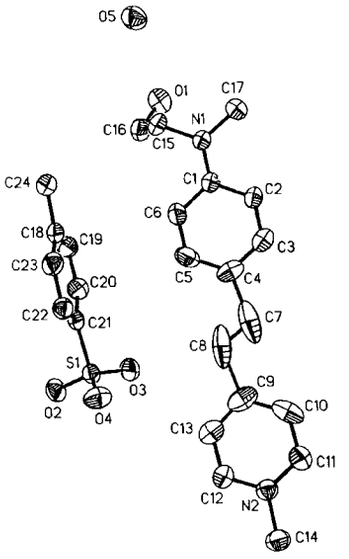

Fig. 2 Molecular structure of HMASPS.

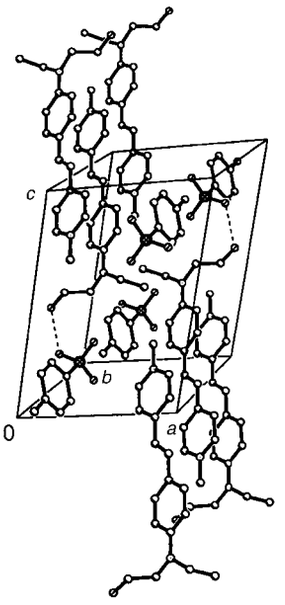

Fig. 3 Packing diagram for HEASPS.

C8–C9 consists of isolated single and double bonds. This deviation from conjugacy may not be intrinsic because crystallographic disorder appears in C7 and C8 (see Fig. 2). In short, both the HMASPS cation and the HEASPS cation are highly π-conjugated or π-delocalized systems. We consider that this structural characteristic is a necessary condition for two-photon absorption and up-conversion emission.

As positively charged molecules, the HMASP cation and the HEASP cation possess very large dipole moments. We believe that the polarity is another important structural factor for up-conversion lasing. It is known that the TPA cross section is proportional to the imaginary part of the third-order nonlinear optical coefficient Im γ (That is why TPA is known as a third-order nonlinear process). Kogej *et al.* further divided the Im γ expression into three terms.[18] The most dominant one is the dipolar term which is similar to that of the simplified two-state expression for β (the second-order nonlinear optical coefficient) and is not vanishing only for noncentrosymmetric systems.

The polar toluene-*p*-sulfonate anions in both crystals adopt a planar configuration too. We believe that the toluene-*p*-sulfonate anions also make some contribution to TPA. In HMASPS and HEASPS, the anion plane is almost perpendicular to the cation plane with the dihedral angles of 86.3° in the former and of 75.1° in the latter.

2 Single-photon and two-photon excited fluorescence

The two-photon fluorescence spectra were recorded by using a passively mode-locked Nd : YAG laser as pump source, and a single-scan streak camera (Hamamatsu Model C1587) together with a polychromator as a recorder. The pulse duration of the Nd : YAG laser is 50 ps. Single-photon fluorescence was excited by a Hg lamp at 435.8 nm and the corresponding emission spectra were recorded by the above streak camera. DMF was used as solvent with concentrations of 7.53×10^{-2} M for HMASPS and 3.72×10^{-2} M for HEASPS. As mentioned above, no linear absorption occurs in the spectral range from 600 nm to 2000 nm, so upon irradiation with the laser pulse at 1064 nm, the sequential stepwise absorption excited emission can be excluded and the strong frequency up-converted fluorescence can be assigned to a simultaneous two-photon absorption mechanism. From Fig. 6 and Fig. 7, one can see that single-photon-excited fluorescence peaks for HMASPS and HEASPS are located at 632 nm and 630 nm respectively, and the two-photon-excited fluorescence peaks for HMASPS and HEASPS are located at 638 nm, which are about 7 nm red-shifted as compared to those of their single-photon counterparts.

3 The TPP lasing spectra and TPP lasing energy conversion efficiency

In TPP lasing experiments, the 1064 nm, 50 ps pulse from a passively mode-locked Nd : YAG laser was adopted as pump source. Through a $f=7$ cm lens, the pump beam was focused vertically onto the center of a 1 cm path quartz cell that was full of solution sample. The lasing output beam was dispersed by a polychromator and the spectra were recorded by a streak camera (Hamamatsu Model C1587).

Fig. 8 shows the narrow TPP lasing spectra of HMASPS and HEASPS in DMF solution. The peak positions are at 626 nm (for HMASPS) and 624 nm (for HEASPS) respectively with a FWHM of ~25 nm. By comparing Fig. 8 with Fig. 6 or Fig. 7, we can see that the TPP fluorescence peaks are red-shifted by ~13 nm compared with their corresponding TPP lasing peak positions. To identify whether this red-shift is common to other systems, we have recorded the TPP fluorescence spectrum and lasing spectrum of ASPI[19] using the same optical set-up and have found a similar red-shift of about 17 nm in benzyl alcohol solution (see Fig. 9). This result is quite different from that reported in reference 19. From Fig. 9, one can see that the TPP lasing peak is at a shorter wavelength than the TPP fluorescence peak. One may also say the lasing peak is blue-shifted. To identify which peak is moveable, we have carried out a series concentration varying experiment and found out that the lasing peak position was basically fixed while the fluorescence peak position was variable. So the phrase "red-shift" is more rational. This red-shift can be explained by reabsorption based on the following facts. (1) There exists some

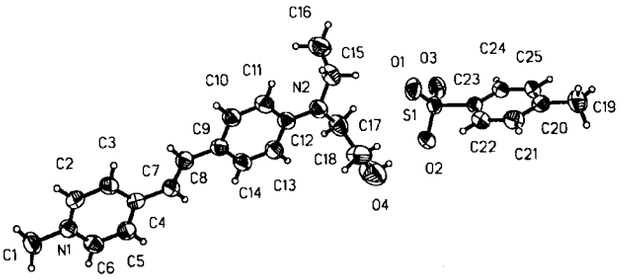

Fig. 4 Molecular structure of HEASPS.

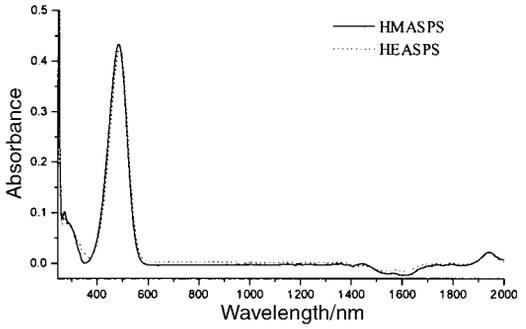

Fig. 5 UV–vis–near-IR absorption spectra of HMASPS and HEASPS in ethanol with the same concentration of 1.00×10^{-5} M.

overlap between the long wavelength side of the absorption band (see Fig. 5) and the short wavelength side of the fluorescence band (see Fig. 6 and 7). The higher the concentration of the solution, the more intense the absorption, and indeed a greater red-shift of the TPP fluorescence peak has been observed. (2) All TPP fluorescence peaks in Fig. 6, 7 and 9 are asymmetric with their left part seeming to be cut off.

Apart from the solution concentration, another factor to influence the position of the TPP lasing peak is the pumping pulse. At the same concentration in benzyl alcohol, the lasing peak of ASPI in our ps pulse set-up is at 613 nm, while that of ASPI by a ns pulse was reported to be at 623 nm.[18] This difference may be also explained by reabsorption. The lasing peak is very narrow and its overlap with the absorption band is almost negligible. However, the tendency of reabsorption, if it exists, should be more effectively overcome by a ps pulse compared to the case of a ns pulse because shorter pump pulses possess stronger pump power.

Another mode-locked Nd : YAG laser with a pulse duration of 50–90 ps was used to measure the lasing output/input intensity curves for HMASPS and HEASPS at the fixed concentration of 5.00×10^{-2} M in DMF solution (see Fig. 10). During the experiment, a laser energy meter (Rj-7200, Laser Precision Corp.) with double detectors was used. One detector was used as the monitor for the pump energy and the other was used to detect the up-conversion lasing energy.

Fig. 11 shows the lasing output/input intensity curves for HMASPS and HEASPS solutions in DMF. From Fig. 11, one can see that the output energy of the two samples increases as the pump level increases. Under exactly the same experimental conditions, the overall energy conversion efficiency is 8.4% for HMASPS (output/input energy is 0.169 mJ/2.02 mJ), 9.1% for

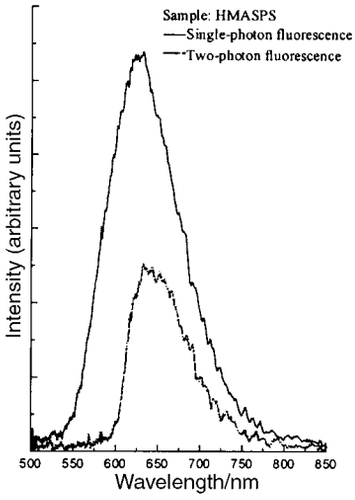

Fig. 6 Single-photon (of 435.8 nm from a Hg lamp) and two-photon (of 1064 nm from a mode-locked Nd : YAG laser) excited fluorescence spectra of 7.53×10^{-2} M HMASPS in DMF.

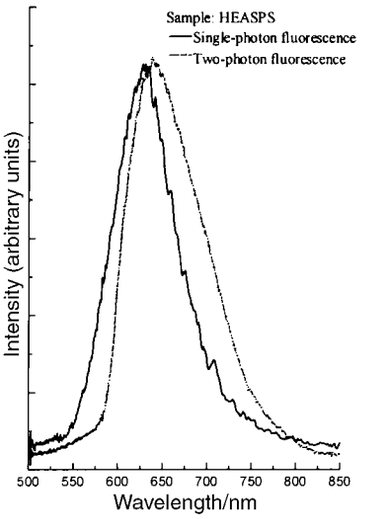

Fig. 7 Single-photon (of 435.8 nm from a Hg lamp) and two-photon (of 1064 nm from a mode-locked Nd : YAG laser) excited fluorescence spectra of 3.72×10^{-2} M HEASPS in DMF.

HEASPS (output/input energy is 0.173 mJ/1.90 mJ). The pumping energy at the lasing threshold was measured to be 0.24 mJ for both HMASPS and HEASPS. In order to compare the output/input characters of our samples with the known up-conversion lasing dye ASPI, the efficiency of a 0.05 M ASPI solution in DMF has also been measured under exactly the same experimental conditions. The conversion efficiency of ASPI is 7.1% (output/input energy is 0.149 mJ/2.10 mJ). From the above results, we can draw the following conclusions. (1) The efficiency of HEASPS is higher than that of HMASPS. (2) The up-conversion efficiencies of HMASPS and HEASPS are higher than that of ASPI. Although the position of TPP lasing depends on the solution concentration and on the pumping source as well as the solvent, it does not depend on the anonic counterion. The counterion influences the FWHM of the TPP lasing peaks, for the FWHM of ASPI–benzyl alcohol solution was measured to be 7.7 nm while that of HMASPS–benzyl alcohol solution is 9.6 nm at the same concentration of 1.5×10^{-2} M and under the same ps pumping source. The higher efficiency of HMASPS compared with ASPI is phenomenally related to the broader width of the peak of TPP lasing. The polar aromatic toluene-*p*-sulfonate has indeed some influence on the up-conversion efficiency as well as on some spectroscopic characteristics. The exact role which the

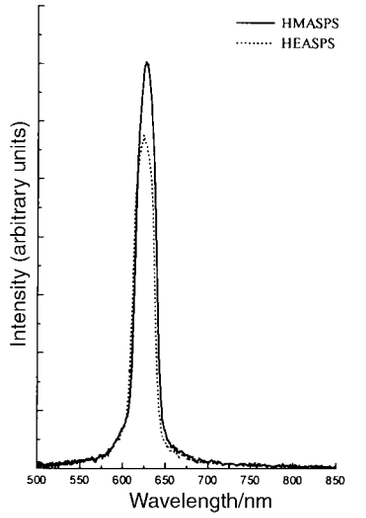

Fig. 8 Two-photon pumped lasing spectra of 7.53×10^{-2} M HMASPS–DMF solution and 3.72×10^{-2} M HEASPS–DMF solution.

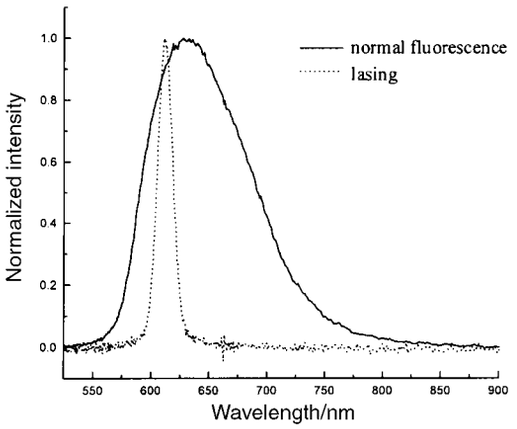

Fig. 9 Two-photon (of 1064 nm from a mode-locked Nd : YAG laser) excited fluorescence and lasing spectra of 0.014 M ASPI–benzyl alcohol solution.

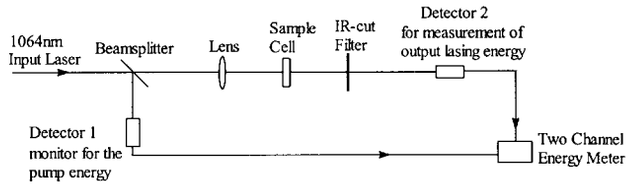

Fig. 10 Experimental set-up for measurement of lasing output/input energies.

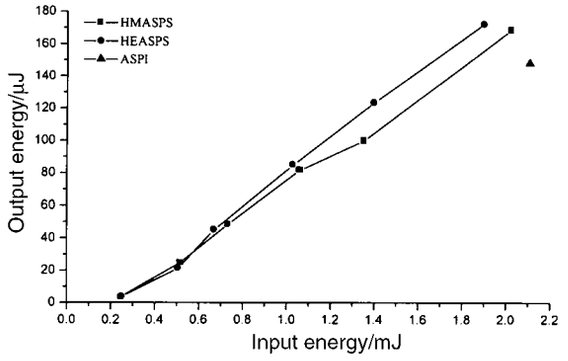

Fig. 11 The output/input curves of HMASPS–DMF and HEASPS–DMF solutions at the same concentration of 5.00×10^{-2} M. For comparison output/input data of an ASPI–DMF solution of the same concentration have also been indicated.

counterion plays is still not very clear and is under investigation.

Conclusion

Two new stable organic salts, HMASPS and HEASPS, have been synthesized. Their structures have been determined. Strong two-photon pumped (1064 nm) fluorescence and lasing around 630 nm were found for HMASPS and HEASPS solution. To our knowledge, HMASPS and HEASPS are among the few laser dyes with the highest up-conversion efficiency. Comparing HMASPS and HEASPS with ASPI, the polar aromatic toluene-*p*-sulfonate anion also has some influence on the TPA as well as on the TPP up-conversion emission process.

Acknowledgements

This work was supported by a grant for state key program of China and by the National Nature Science Foundation of China.

References

1 W. Denk, J. H. Strickler and W. W. Webb, *Science*, 1990, **248**, 73.
2 J. H. Strickler and W. W. Webb, *Opt. Lett.*, 1991, **16**, 1780.
3 D. A. Parthenopoulos and P. M. Rentzepis, *Science*, 1989, **245**, 843.
4 B. H. Cumpston, S. P. Ananthavel, S. Barlow, D. L. Dyer, J. E. Ehrlich, L. L. Erskine, A. A. Heikal, S. M. Kuebler, I.-Y. Sandy Lee, D. McCord-Maughon, J. Qin, H. Röckel, M. Rumi, X. L. Wu, S. R. Marder and J. W. Perry, *Nature* (London), 1999, **398**, 51.
5 S. Maruo, O. Nakamura and S. Kawata, *Opt. Lett.*, 1997, **22**, 132.
6 E. S. Wu, J. H. Strickler, W. R. Harrell and W. W. Webb, *Proc. SPIE–Int. Soc. Opt. Eng.*, 1992, **1674**, 776.
7 C. F. Zhao, G. S. He, J. D. Bhawalkar, C. K. Park and P. N. Prasad, *Chem. Mater.*, 1995, **7**, 1979.
8 G. S. He, L. X. Yuan, Y. P. Cui, M. Li and P. N. Prasad, *J. Appl. Phys.*, 1997, **81**, 2529.
9 G. S. He, L. X. Yuan, P. N. Prasad, A. Abbotto, A. Facchetti and G. A. Pagani, *Opt. Commun.*, 1997, **140**, 49.
10 G. S. He, K. S. Kim, L. X. Yuan, N. Cheng and P. N. Prasad, *Appl. Phys. Lett.*, 1997, **71**, 1619.
11 G. S. He, R. Signorini and P. N. Prasad, *IEEE J. Quantum Electron.*, 1998, **34**, 7.
12 J. D. Bhawalkar, G. S. He, C. K. Park, C. F. Zhao, G. Ruland and P. N. Prasad, *Opt. Commun.*, 1996, **124**, 33.
13 G. S. He, R. Signorini and P. N. Prasad, *Appl. Opt.*, 1998, **37**, 5720.
14 H. Stiel, K. Tenchner, A. Paul, W. Freyer and D. Leupold, *J. Photochem. Photobiol. A: Chem.*, 1994, **80**, 289.
15 M. Albota, D. Beljonne, J. L. Bredas, J. E. Ehrlich, J. Y. Fu, A. A. Heikal, S. E. Hess, T. Kogej, M. D. Levin, S. R. Marder, D. McCord-Maughon, J. W. Perry, H. Röckel, M. Rumi, G. Subramaniam, W. W. Webb, X. L. Wu and C. Xu, *Science*, 1998, **281**, 1653.
16 B. A. Reinhardt, L. L. Brott, S. J. Clarson, A. G. Dillard, J. C. Bhatt, R. Kannan, L. X. Yuan, G. S. He and P. N. Prasad, *Chem. Mater.*, 1998, **10**, 1863.
17 C. F. Zhao, C. K. Park, P. N. Prasad, Y. Zhang, S. Ghosal and R. Burzynski, *Chem. Mater.*, 1995, **7**(6), 1237.
18 T. Kogej, D. Beljonne, F. Meyers, J. W. Perry, S. R. Marder and J. L. Brédas, *Chem. Phys. Lett.*, 1998, **298**, 1.
19 G. S. He, Y. P. Cui, J. D. Bhawalkar, P. N. Prasad and D. D. Bhawalkar, *Opt. Commun.*, 1997, **133**, 175.